

Trivial bundle embeddings for learning graph representations

Zheng Xie, Xiaojing Zuo, Yiping Song

Received: date / Accepted: date

Abstract Embedding real-world networks presents challenges because it is not clear how to identify their latent geometries. Embedding some disassortative networks, such as scale-free networks, to the Euclidean space has been shown to incur distortions. Embedding scale-free networks to hyperbolic spaces offer an exciting alternative but incurs distortions when embedding assortative networks with latent geometries not hyperbolic. We propose an inductive model that leverages both the expressiveness of GCNs and trivial bundle to learn inductive node representations for networks with or without node features. A trivial bundle is a simple case of fiber bundles, a space that is globally a product space of its base space and fiber. The coordinates of base space and those of fiber can be used to express the assortative and disassortative factors in generating edges. Therefore, the model has the ability to learn embeddings that can express those factors. In practice, it reduces errors for link prediction and node classification when compared to the Euclidean and hyperbolic GCNs.

1 Introduction

Social networks, molecular graph structures, recommender systems—all of these domains and many more can be readily modeled as graphs, which capture interactions between individual units. Graph data extensively exist in computer science and related fields. To extract structural information from graphs, traditional machine approaches often rely on summary graph statistics, such as degree and clustering coefficient, or carefully engineered features to measure local neighborhood structures.

Z. Xie, X. Zuo, Y. Song
College of Liberal Arts and Sciences, National University of Defense Technology, Changsha, China.
E-mail: xiezheng81@nudt.edu.cn

In computer science and network science, a network can be defined as a graph in which nodes and edges can have features. Network geometry aims at making a paradigmatic shift in our understanding of complex network structures by revealing their hidden metric. It can be used to design inductive prediction models for network evolution, and to deal with the analysis of high-order networks whose node feature vectors are available. There has been a range of approaches to learning the geometric representations of networks. They encode node and subgraph information as points in geometry, decode the points to express network structures, and then obtain embeddings by optimizing a loss that measures the difference between the decoded structures and the original structures.

Graph convolutional neural networks (GCNs) are effective models for representation learning in graphs, where nodes of the graph are embedded into points in Euclidean space (Hamilton et al. 2017; Kipf and Welling 2017; Veličković et al. 2017; Xu et al. 2019). When considering a scale-free network whose degree distribution follows a power law, embedding those nodes having very many neighbors to the Euclidean space incurs distortions because unconnected nodes would crowd together (Sala et al. 2018; Sarkar 2011).

When assuming hyperbolic geometry underlies networks, the network features scale-free and high-clustering emerge naturally as simple reflections of the negative curvature and metric property of the underlying hyperbolic geometry (Krioukov et al. 2010). For instance, Poincaré embeddings outperform its Euclidean analogs significantly on networks with latent hierarchies (Nickel and Kiela 2017). Extending GCNs to hyperbolic geometry has been shown to provide more faithful embeddings. These hyperbolic variants are state-of-the-art models, can take into account features of nodes and edges, have the inductive capability, and thus provide exciting improvements.

The evolution of networks is driven by nodes' preference of choosing which nodes to connect. A network shows assortativity if its nodes prefer to associate with others who are like them, and shows disassortativity if its nodes prefer to associate with those who are different. Social networks are usually found to be assortative by most characteristics, empirically showing that nodes tend to connect to other nodes with similar degree values. Technological and biological networks typically show disassortativity, as high degree nodes tend to attach to low degree nodes (Newman 2003).

In real-world networks, some nodes show assortativity, and others disassortativity. For instance, the dichotomous phenomenon exists in node clustering and degree assortativity of coauthorship networks, which are distinct from small degree nodes to large degree ones. While applying the Euclidean and hyperbolic GCNs to these networks poses a challenge: which part of nodes needs to be embedded to the Euclidean spaces, and which to hyperbolic.

We solve the above challenge by embedding networks into trivial bundles. We propose a graph representation learning model, trivial bundle graph convolution network (TB-GCN), which combines the expressiveness of GCNs and trivial bundles to learn improved representations for networks in inductive settings. TB-GCN captures both the assortativity and disassortativity in nodes'

preference of choosing which nodes to connect. TB-GCN achieves error reduction on link prediction (LP) and node classification (NC) tasks in comparison to the Euclidean and hyperbolic GCNs.

2 Background

2.1 Fiber bundles

A fiber bundle is a space that is locally a product space but globally may have a different topological structure. Specifically, the similarity between a bundle E and a product space $B \times F$ is described through a continuous surjective map, $\pi: E \rightarrow B$, that in small regions of E behaves just like a projection from corresponding regions of $B \times F$ to B . The map π , called the projection or submersion of the bundle, is regarded as part of the structure of the bundle. The space E is known as the total space of the fiber bundle, B as the base space, and F the fiber. In the trivial case, E is just $B \times F$, and the map π is just the projection from the product space to the first factor. This is called a trivial bundle. We refer the readers to Ref.(Steenrod 2016) for a thorough discussion of fiber bundles.

2.2 Graph representation learning

We consider graph representation learning on a graph $G = (V, E, X^0)$, where V is the node set, E is the edge set, and $X^0 \in R^{|V| \times d}$ is the matrix of input node features. The i -column (x_i^0) of X^0 is the feature of node $i \in V$ valued as a d -dimensional vector and the superscript 0 indicates the first layer. When without input node features, (x_i^0) is the one-hot vector with the value of the i -th entry being 1 and all other entries being 0. Here, the goal in graph representation learning of TB-GCN is to learn a mapping f which embeds nodes to a trivial bundle $E = B \times F$ (Fig.1). These embeddings should capture both structural and semantic information and can then be used as input for downstream tasks such as node classification and link prediction.

2.3 Euclidean graph convolution networks

For the implementation here, we only use the Euclidean GCNs to achieve this aim. Let $G = (V, E)$ be a graph with node features $X^{(0)} \in R^{N \times m}$. Let $(W^{(l)}, b^{(l)})$ be weights and bias parameters for layer l , and $\sigma(\cdot)$ be a non-linear activation function. General GCN message passing rule at layer l for node i then is defined as follows:

$$X^{(l+1)} = \sigma \left(\tilde{A} \left(X^{(l)} W^{(l)} + b^{(l)} \right) \right), \quad (1)$$

where there exist different ways to compute the aggregation matrix \tilde{A} based on network data.

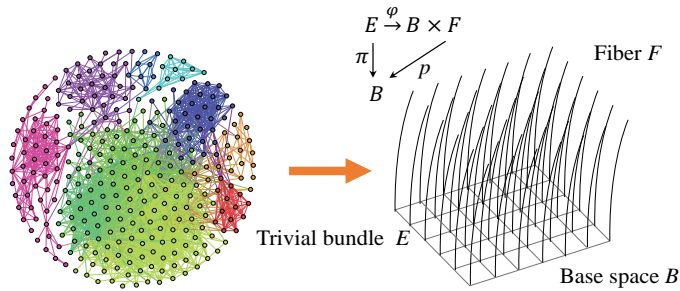


Fig. 1: The illustration of trivial bundle embeddings.

3 Literature review

3.1 Shallow Euclidean embeddings

The early Euclidean embeddings for graphs are based on matrix-factorial approaches, directly inspired by the techniques of dimensional reduction. The idea of these approaches is that considering a graph’s adjacency matrix, for example, the user-item interaction matrix of a bipartite graph, it is decomposed into the product of two lower dimensionality matrices, then its nodes are represented as vectors in a lower-dimensional vector space. These approaches, such as singular value decomposition (SVD) and nonnegative matrix factorization (NMF)(Lee and Seung 1999), are applied in recommender systems(Dhillon and Sra 2005), text clustering(Gemulla et al. 2011), etc. They belong to principal components analysis (PCA)(Dunteman 1989), however, they do not consider the intrinsic geometry of the data. Laplacian eigenmaps are based on the assumption that data are sampled from an intrinsic geometry lying in a high-dimensional space. They build a graph from k -nearest neighbors computed from the original data, which is a discrete approximation of its intrinsic geometry. Minimizing a cost function based on the graph ensures that points close to each other on the manifold are mapped close to each other in the low-dimensional space, preserving local distances(Belkin and Niyogi 2001).

3.2 Shallow non-Euclidean embeddings

Riemannian optimization has been used to learn embeddings to map graphs into Poincaré ball(Nickel and Kiela 2017; Tifrea et al. 2019) and Lorentz space(Nickel and Kiela 2018). These models outperform the Euclidean embedding methods on graph reconstruction and link prediction for scale-free networks, and have been applied to text analysis(Tifrea et al. 2019; Dhingra et al. 2018). The maximum likelihood estimation also has been used to embed graphs to hyperbolic space(Papadopoulos et al. 2014; Wang et al. 2016). Coalescent embedding based on nonlinear dimension reduction algorithms offers a

fast embedding in the hyperbolic space even for large graphs(Muscoloni et al. 2017).

3.3 Deep Euclidean embeddings

The methods reviewed above are shallow embedding approaches. They cannot share parameters for nodes, the number of parameters growing linearly with the number of nodes, fail to leverage node attributes, and are inherently transductive, not suitable for dynamic data. The Euclidean GCNs offer inductive approaches to learning embeddings from input graph structure as well as node features(Xu et al. 2019). These models can be designed as inductive ones(Hamilton et al. 2017), as semi-supervised ones for classification task(Kipf and Welling 2017), modified to use gated recurrent units(Li et al. 2016) or attention mechanism(Veličković et al. 2017), and applied to recommender systems(Ying et al. 2018). While resolving the disadvantages of shallow embeddings, these approaches lead to distortions when applied to scale-free networks.

3.4 Deep non-Euclidean embeddings

Based on hyperbolic neural networks(Ganea et al. 2018) and hyperbolic attention networks(Gulcehre et al. 2019), GNNs have been extended to hyperbolic geometry, known as HGNNs, for graph classification tasks(Liu et al. 2019), link prediction, and node classification tasks(Chami et al. 2019). Learning embeddings to products of three kinds of spaces, namely spherical, hyperbolic, and Euclidean has been shown to outperform the embeddings to single Euclidean or hyperbolic spaces(Gu et al. 2018). Riemannian optimization is used to jointly learn the curvature and the embedding in the product space. Although our work also discuss the embeddings to product space, the loss function is different. For sequences of dimensions $s_1, s_2, \dots, s_m, h_1, h_2, \dots, h_n$, and e , the embedding space is $P = S^{s_1} \times S^{s_2} \times \dots \times S^{s_m} \times H^{h_1} \times H^{h_2} \times \dots \times H^{h_n} \times E^e$; the loss function in Ref.(Gu et al. 2018) is $L(x) = \sum_{1 \leq i < j \leq n} |d_P(x_i, x_j)^2 / |d_G(X_i, X_j)^2 - 1|$, where $d_P(p, q) = \sum_{i=1}^{s_m} d_{S_i}(p, q) + \sum_{j=1}^{h_n} d_{H_j}(p, q) + d_E(p, q)$, and $d_G(X_i, X_j)$ is the given graph distance.

4 TB-GCN architecture

We propose TB-GCN to embed networks into trivial bundles, representing the assortativity and disassortativity in the preference of choosing which nodes to connect. This is a perspective different from HGCNs, which are proposed based on the assumption that the underlying geometry of scale-free networks is hyperbolic. That is, the rationality of HGCNs is based on the scale-free feature of networks. Given a network with a fixed degree distribution, we can tune its

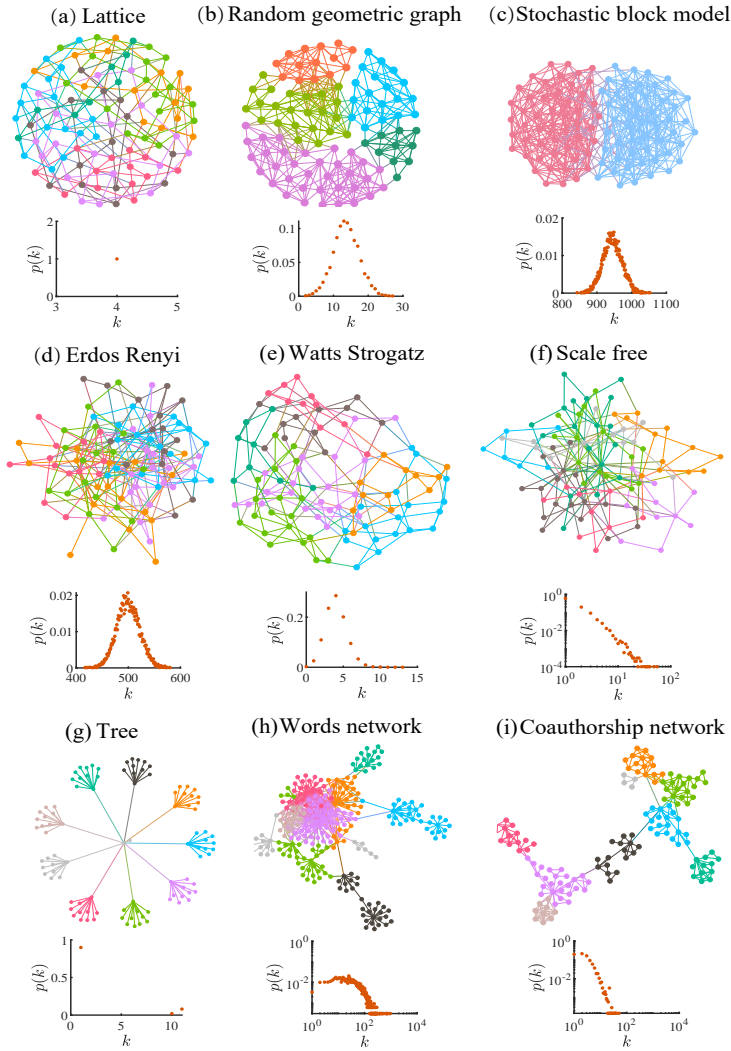


Fig. 2: Typical real-world and synthetic networks and their degree distribution. The degree distributions of the networks from different types can belong to the same class.

assortativity coefficient by rewiring a fraction of connections (Newman 2003). Fig. 2 shows the assortativity coefficient is free of the feature of the degree distribution, such as scale-free, Poisson, and their mixture. Therefore, discussing which space is suitable to embed a network with a given assortativity coefficient has its own meaning.

We assume that both assortativity and disassortativity exist in the preference of choosing which nodes to connect. We learn embeddings of network

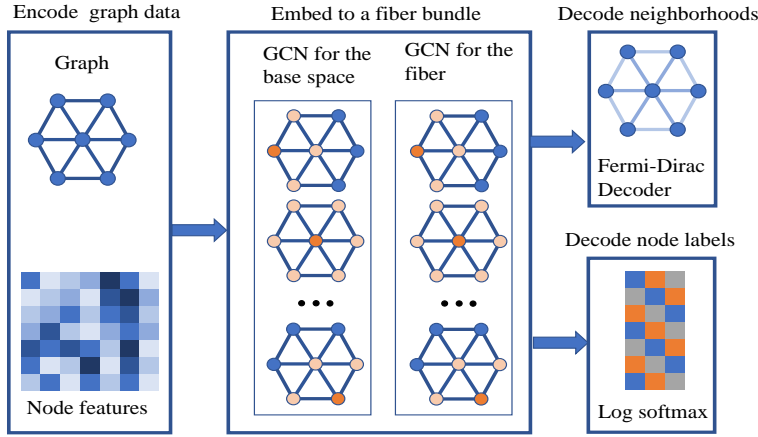


Fig. 3: The architecture of TB-GCN. The originality is the decoders, which represent the assortativity and disassortativity in nodes' preference of choosing which nodes to connect.

data such that their coordinates of base space can be used to decode the assortativity and their coordinates of fiber used to decode the disassortativity. There exist multiple choices of base space and fiber, for example the Poincaré ball for base space and the Euclidean for fiber. In the following, we will consider a simple case, namely, both are the Euclidean space, as it is enough to represent the assortativity and disassortativity. The architecture of TB-GCN is described within the encoder-decoder framework (Fig. 3), The originality of TB-GCN is its decoders, which represent the assortativity and disassortativity. The model is trained by minimizing the loss function of a given task.

4.1 Encoders

We describe our main embedding space: $E = B \times F$, where $B = \{x_1, \dots, x_m\}$ and $F = \{y_1, \dots, y_n\}$. Given a graph $G = (V, E)$ and input Euclidean features $\{X^{(0)} \in \mathbb{R}^{N \times m}, Y^{(0)} \in \mathbb{R}^{N \times n}\}$. Let $\tilde{A} = D^{-\frac{1}{2}}(A + I)D^{-\frac{1}{2}}$, where I is the identity matrix, A the adjacency matrix, and $D = (\sum_j (A_{ij} + I_{ij}))$. TB-GCN stacks multiple Euclidean graph convolution layers for the base space and fiber with the following layer-wise propagation rule:

$$\begin{cases} X^{(l+1)} = \sigma \left(\tilde{A} \left(X^{(l)} W_B^{(l)} + b_B^{(l)} \right) \right), \\ Y^{(l+1)} = \sigma \left(\tilde{A} \left(Y^{(l)} W_F^{(l)} + b_F^{(l)} \right) \right). \end{cases} \quad (2)$$

Here $W_{B,F}^{(l)}$ and $b_{B,F}^{(l)}$ are the layer-specific trainable weight matrices and biases for the base space B and F respectively; $\sigma(\cdot)$ denotes an activation function, such as the $\text{ReLU}(\cdot) = \max(0, \cdot)$; $X^{(l)} \in \mathbb{R}^{N \times m}$ and $Y^{(l)} \in \mathbb{R}^{N \times n}$ are the

matrices of activations in the l -th layer; $X^{(0)}$ and $Y^{(0)}$ are input. Note that our model is a multi-view model if $X^{(0)} \neq Y^{(0)}$, and not if $X^{(0)} = Y^{(0)}$.

4.2 Decoders

If the objective is the probability of existing an edge between two given nodes, We use the Fermi-Dirac decoder to decoder the probability scores for edge $l = (p, q)$:

$$P(l \in E) = \left(e^{(d(p,q)-r)/t} + 1 \right)^{-1}, \quad (3)$$

where $d(p, q)$ is a value positively correlated to $P(l \in E)$, r and t are hyper-parameters. One originality of our model is defining

$$d(p, q) = \left(\sum_{i=1}^m (x_i(p) - x_i(q))^2 \right) \left(\sum_{j=1}^n (y_j(p) + y_j(q))^2 \right). \quad (4)$$

The first factor represents the assortativity, and the second disassortativity, and thus $d(p, q)$ both. That is, the role of base space embeddings is used to decode the assortativity and the role of fiber embeddings is to the disassortativity. Note that Eq.4 does not need $m = n$.

Different from the product space embeddings (Gu et al. 2018), the decoder here not only considers the assortativity factor (the smaller the distance between two nodes, the more likely they connect) but also considers the disassortative factor (the larger the distance between two nodes, the more likely they connect). The roles of the first and second terms in Eq.4 are equal. Which term or both being activated depends on the assortativity, disassortativity, or their mixture of data.

If the objective is a vector that is used to represent the label or type of a node, we decode the vector by subtracting, dividing, and multiplying each element of the last layer of base space $X^{(L)}$ by the corresponding element of the last layer of fiber $Y^{(L)}$ respectively. The subtracting and dividing operations represent the antagonism of the base space embeddings and fiber embeddings, meanwhile, the multiplying operation represents their complementarity. Then, in those situations, the dimension of fiber should be equal to that of base space.

4.3 Two Tasks

Link prediction. For LP tasks, We use negative sampling to train TB-GCN by minimizing the cross-entropy loss. Let E^+ and E^- be the positive and negative training edge sets. The loss is

$$L_{\text{LP}} = - \sum_{l \in E^+} \frac{\log P(l \in E^+)}{|E^+|} - \sum_{l \in E^-} \frac{\log(1 - P(l \in E^-))}{|E^-|}. \quad (5)$$

Network	Nodes	Edges	Classes	Features	Assortativity
CORA	2708	5429	7	1433	-0.0659
PUBMED	19717	44327	3	500	-0.0436
AIRPORT	3188	18631	4	4	-0.0157
DISEASE-CN	1044	1043	2	1000	-0.5441

Table 1: Statistics of the networks used for node classification tasks.

Node classification. For NC tasks, we have three ways to decode the embeddings as vectors, namely subtracting, dividing, and multiplying, and we denote the corresponding models as TB-GCN-SUB, -DIV, and -MUL respectively. Therefore, the dimension of fiber should be equal to that of base space for NC tasks, namely $m = n$.

We perform the Euclidean multinomial logistic regression on outputs, and then train TB-GCN by minimizing the negative log likelihood loss

$$L_{\text{CN}} = - \sum_{i \in N^{\text{T}}} \frac{\log P_{c(i)}(i)}{|N^{\text{T}}|}, \quad (6)$$

where $P_{c(i)}(i)$ is the probability that node i is correctly classified into its class $c(i)$. We also add a link prediction regularization objective in node classification tasks, to encourage embeddings at the last layer to preserve the graph structure. In this situation, the loss is

$$L_{\text{CNLP}} = \gamma L_{\text{CN}} + (1 - \gamma) L_{\text{LP}}, \quad (7)$$

where $\gamma \in [0, 1]$ weights the role of preserving the graph structure in NC tasks.

Computational complexity. The number of multiplications in Eq. (2) is $N^2(m + n + 1) + N(m^2 + n^2)$, and thus the number of multiplications of propagating K layers is $KN^2(m + n + 1) + KN(m^2 + n^2)$. Therefore, the complexity of TB-GCNs is on par with that of GCNs. It can be scaled to large graphs as GCNs do.

5 Experimental setup

5.1 Datasets

We use a variety of datasets that we detail in Tables 1 and 2. We compute their assortativity coefficient, an index that measures the degree of assortativity a graph is. The lower, the more disassortativity is the network. The random geometric graph and coauthorship networks have a positive assortativity coefficient, and trees negative.

1. **Citation networks.** CORA(Sen et al. 2008) and PUBMED(Namata et al. 2012) are standard benchmarks describing citation networks, where nodes represent papers, edges represent citations between them, and node labels are academic areas.

Name	Nodes	Edges	Assortativity
WORD-TREE	4679	128974	-0.1128
CA-HEP	11204	117619	0.6295
CA-INF	13102	19239	0.1627
WIKI-VOTE	7066	100736	-0.0833
DISEASE-LP	2665	2664	-0.6135
WS	1600	3200	0.0116
PA	1000	7000	-0.0219
BSM	1000	52411	-0.0100
RGG	1000	14233	0.5423
TREE	1000	999	-0.8223
TREE+LATTICE	1000	2355	-0.0441
TREE+RGG	1000	2407	-0.0312

Table 2: Statistics of the networks used for link prediction tasks.

2. **Coauthorship networks.** CA-HEP is standard benchmark describing collaboration networks covering papers in the period from Jan 1993 to Apr 2003(Leskovec et al. 2007), where nodes represent authors, edges represent coauthorship between them. CA-INF downloaded from Web of Science², which covers authors’ collaborations in the papers of three accredited journals of informetrics, namely the Journal of the Association for Information Science and Technology, Journal of Informetrics, and Scientometrics during Jan 2006–Dec 2002. If the paper is co-authored by k authors this generates a completely connected subgraph on k nodes.

3. **Tree-like networks.** Disease-CN and -LP are tree-like networks generated by the SIR disease spreading model(Anderson and May 1992), where the label of a node is whether the node was infected or not and node features indicate the susceptibility to the disease. WORD-TREE is a word-attention network containing the word branches of the PNAS papers published in 2015, which are generated by the model in Ref. (Xie 2021).

4. **Flight networks.** AIRPORT is a transductive dataset where nodes represent airports and edges represent the airline routes as from Open Flights.org. The network has geographic information (longitude, latitude, and altitude), and the GDP of the country where the airport belongs to. Node labels are the populations of airports’ country(Chami et al. 2019).

5. **Vote network.** WIKI-VOTE contains all the Wikipedia voting data from the inception of Wikipedia till 2008.01(Leskovec et al. 2010). Nodes in the network represent Wikipedia users and a directed edge from node i to node j represents that user i voted on user j .

6. **Synthetic networks.** WS is generated by the Watts-Strogatz model, where the dimension of the lattice is 2, the size of the lattice along all dimensions is 10, the value giving the distance within which two nodes will be connected is 1, and the rewiring probability is 0.1. SCALE-FREE is a scale-

² <http://www.webofknowledge.com>

free network, and the exponent of its out-degree distribution is 2.1. BSM is generated by the stochastic block model, where the number of blocks is 2, the number of nodes in each block is 500, the matrix giving the connection probabilities for different blocks is $[0.2, 0.01]$. RGG is a random geometric graph in a disc with radius 1, and two nodes will connect if their distance is less than 0.03. TREE is a network in which almost all nodes have the same number of children 10. TREE+LATTICE is the TREE with edges generated by lattice model with dimensional list $[10, 10]$. TREE+RGG is the combination of TREE and RGG.

5.2 Baselines

Since the deep methods have been shown to outperform shallow methods, we only consider six state-of-the-art deep methods: Graph attention networks (GAT)(Veličković et al. 2017), Graph convolution networks (GCN)(Kipf and Welling 2017), Hyperboloid and Poincaré embeddings (Nickel and Kiela 2017) with hyperbolic neural networks (Ganea et al. 2018) and hyperbolic graph convolution networks(Chami et al. 2019) respectively (HNN-HYP, HNN-POI, HGCN-HYP, HGCH-POI). We conjecture that TB-GCN will outperform on the networks with both of the assortative and disassortative existing in nodes' preference of choosing which nodes to connect.

The propose of our model is to show that compared with Euclidean and hyperbolic spaces, trivial bundles would be suitable for GCN embedding the complex networks with both of the assortative and disassortative existing in nodes' preference of choosing which nodes to connect. We mainly compared it with GCNs. Meanwhile, assertion error happens when running GATs on some datasets, e.g., CORA. Therefore, some state-of-the-art of hyperbolic GATs (Zhu et al. 2020; Zhang et al. 2021) are not chosen as baselines.

5.3 Implementation Details

The hyper-parameters of t and r in Eq. (3), the initial learning rate, weight decay, DropConnect(Wan et al. 2013), the number of layers, and activation functions are the same as HGCN(Chami et al. 2019). The hyper-parameter $\gamma \in \{0.0, 0.25, 0.50, 0.75, 1.0\}$ in the loss (7) is used only for the NC task. The dimension of embedding space is 128 here, but 16 in Ref. (Chami et al. 2019)).

We use early stopping based on validation set performance with the patience of 1,000 epochs and 15,000 the maximum number of epochs to train. We measure performance on the final test set. For fairness, we control the dimensions to be the same (128) for all methods, the dimension of fiber and that of base space to be 64. We use a fixed random seed set 1234. We optimize the considered TB-GCN (note that the base space and fiber are Euclidean), GCN, GAT with Adam Optimizer(Kingma and Ba 2015), and others with RiemannianSGD Optimizer(Bonnabel 2013; Zhang et al. 2016). We open-source our

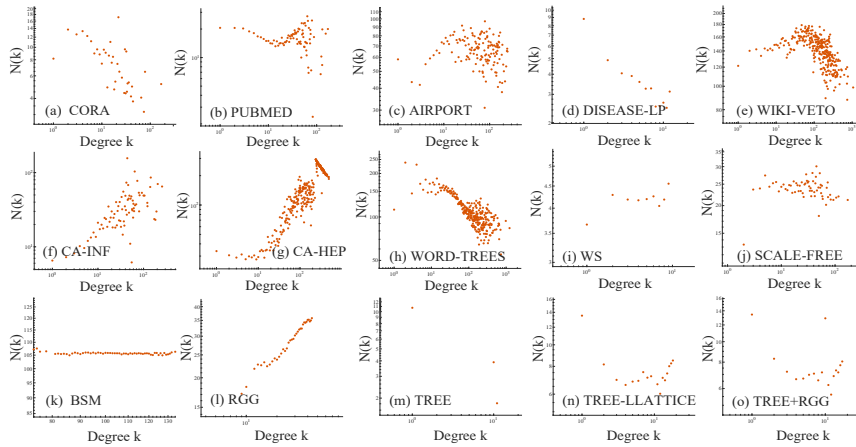


Fig. 4: The average degree $N(k)$ of k -degree nodes' neighbors. The panels show $N(k)$ for the networks in Table 2.

implementation of TB-GCN at Github, which contains the initial settings of hyperparameters of TB-GCN and baselines.

5.4 Evaluation Metric

We evaluate our method on a variety of networks, on both NC and LP tasks. In LP tasks, we randomly split edges into 85/5/10% for training, validation, and test sets, the same as those in Ref.(Ioffe and Szegedy 2015), and use the node features if exist. For NC tasks, we use 70/15/15% splits for AIRPORT, 30/10/60% splits for DISEASE, and standard splits in Refs.(Kipf and Welling 2017; Yang et al. 2016) with 20 train examples per class for CORA and PUBMED. We use the node features if exist. We evaluate link prediction by measuring the area under the ROC curve (AUC) and average precision (AP) on the test set and evaluate node classification by measuring F1 score.

5.5 Overall Performance

Table 3 reports the performance of TB-GCN with different decoders (-SUB, -DIV, -MUL) and different values of the parameter γ in the loss (7) on NC tasks. The cases with $0 < \gamma < 1$ outperform those with $\gamma = 0$, which means both node features and network topology contribute to NC tasks. TB-GCN-SUB achieves the best performance on two networks, and others on one, which means all of the decoders have their advantages.

Table 4 reports the performance of baseline methods on NC tasks in comparison to the best performance of TB-GCN. It shows that TB-GCN achieves

	γ	CORA	PUBMED	AIRPORT	DISEASE_CN
TB-GCN-SUB	0	0.7880	0.7590	0.9294	0.8734
	0.25	0.7980	0.8030	0.9370	0.8634
	0.50	0.8040	0.7990	0.9313	0.7814
	0.75	0.8050	0.8030	0.9084	0.7005
	1.00	0.1320	0.3890	0.2729	0.8053
TB-GCN-DIV	0	0.6990	0.7080	0.8378	0.7368
	0.25	0.7440	0.7480	0.7805	0.9091
	0.50	0.7460	0.7620	0.7882	0.8974
	0.75	0.7480	0.7670	0.7538	0.8161
	1.00	0.2960	0.5650	0.4351	0.5141
TB-GCN-MUL	0	0.7960	0.7550	0.9160	0.8734
	0.25	0.8060	0.7850	0.9179	0.8596
	0.50	0.8220	0.7780	0.9160	0.8496
	0.75	0.8190	0.7850	0.9160	0.8235
	1.00	0.2450	0.3890	0.1756	0.7401

Table 3: F1 scores of TB-GCN on node classification tasks for the networks in Table 1. We report the performances of TB-GCN with different values of the parameter γ in the loss (7) and different decoders -SUB, -DIV, -MUL.

	TB-GCN	HGCN-HYP	HGCN-POI	HNN-HYP	HNN-POI	GCN	GAT	ERR-RED
CORA	0.8220	0.7740	0.7930	0.5910	0.6070	0.7990	0.7540	0.0230
PUBMED	0.8030	0.7830	0.7770	0.7390	0.7350	0.7570	0.7370	0.0200
AIRPORT	0.9370	0.8511	0.8359	0.7939	0.7767	0.9218	0.8153	0.0152
DISEASE-CN	0.9091	0.7228	0.7714	0.6667	0.6667	0.8444	0.8444	0.0647

Table 4: F1 scores of baselines on node classification tasks for the networks in Table 1. We report the best performance of TB-GCN compared with baselines.

error reduction compared to the best baselines for the four networks considered in Ref. (Chami et al. 2019), especially on DISEASE-CN (error reduction 6%). The variations between the performance of baseline approaches here and the performance in the results are computed by the package "gcn-master" that is downloaded from Github. Ref. (Chami et al. 2019) due to the difference in the dimensions of embedding space (128 here and 16 in Ref. (Chami et al. 2019)).

Table 5 reports the performance of TB-GCN on LP tasks in comparison to the performances of baseline methods. It shows that TB-GCN achieves error reduction compared to the best deep baselines for eight networks in Table 1. The performances of baseline methods on the first four networks here slightly vary from that in Ref. (Chami et al. 2019), which are also due to the difference in hyperparameter settings. HNN-POI outperforms TB-GCN on DISEASE-LP, suggesting that hyperbolic geometry is more suitable for the SIR disease spreading model. TB-GCN outperforms baseline methods on the real-world network WORD-TREES, the synthetic networks TREE, and

Data		TB-GCN	HGCN-HYP	HGCN-POI	HNN-HYP	HNN-POI	GCN	GAT	ERR RED
CORA	AUC	0.9409	0.9196	0.9167	0.9021	0.9409	0.9409	0.9400	0.000
	AP	0.9424	0.9249	0.9286	0.9141	0.9424	0.9424	0.9382	0.000
PUBMED	AUC	0.9588	0.9414	0.9442	0.9619	0.9650	0.9384	0.9439	-0.0062
	AP	0.9586	0.9451	0.9491	0.9569	0.9607	0.9349	0.9415	-0.0021
AIRPORT	AUC	0.9576	0.9332	0.9394	0.9471	0.9316	0.9536	0.9471	0.004
	AP	0.9517	0.9447	0.9415	0.9426	0.9389	0.9473	0.9426	0.0044
DISEASE-LP	AUC	0.6339	0.6159	0.6561	0.7448	0.8033	0.6181	0.6308	-0.1694
	AP	0.6025	0.5998	0.6325	0.7290	0.7705	0.6050	0.6162	-0.1680
WIKI-VETO	AUC	0.9701	0.9525	0.9499	0.9541	0.9579	0.9431	0.9413	0.0122
	AP	0.9653	0.9542	0.9504	0.9556	0.9572	0.9219	0.9223	0.0081
CA-INF	AUC	0.9481	0.8922	0.9153	0.8930	0.9056	0.9357	0.9408	0.0073
	AP	0.9648	0.9386	0.9503	0.9417	0.9469	0.9565	0.9531	0.0117
CA-HEP	AUC	0.9818	0.9757	0.9761	0.9755	0.9782	0.9700	0.9742	0.0036
	AP	0.9860	0.9839	0.9841	0.9832	0.9849	0.9703	0.9744	0.0011
WORD-TREES	AUC	0.8690	0.8668	0.8671	0.8628	0.8652	0.8310	0.8520	0.0019
	AP	0.8498	0.8416	0.8427	0.8371	0.8394	0.8097	0.8323	0.0071
WS	AUC	0.7524	0.7659	0.7075	0.7080	0.7023	0.7356	0.7371	-0.0135
	AP	0.7889	0.7073	0.7685	0.7613	0.7603	0.7646	0.7748	0.0141
SCALE-FREE	AUC	0.6470	0.6669	0.6643	0.6500	0.6589	0.6389	0.6371	-0.0026
	AP	0.6639	0.6807	0.6791	0.6641	0.6739	0.6390	0.6465	0.0016
BSM	AUC	0.7602	0.7613	0.7636	0.7588	0.7614	0.7618	0.7582	-0.0034
	AP	0.6781	0.6810	0.6859	0.6752	0.6817	0.6860	0.6738	0.0078
RGG	AUC	0.9966	0.9969	0.9968	0.9965	0.9964	0.9939	0.9943	-0.0003
	AP	0.9888	0.9893	0.9891	0.9888	0.9887	0.9850	0.9858	-0.0005
TREE	AUC	0.8045	0.6673	0.6650	0.6556	0.6540	0.6389	0.6371	0.1372
	AP	0.7075	0.6800	0.6788	0.6745	0.6700	0.6390	0.6465	0.0275
TREE+LATTICE	AUC	0.9528	0.9141	0.9136	0.9196	0.9208	0.9044	0.9008	0.032
	AP	0.9574	0.9366	0.9361	0.9388	0.9398	0.9189	0.9153	0.0176
TREE+RGG	AUC	0.9172	0.8979	0.8989	0.9027	0.9098	0.8731	0.9040	0.0074
	AP	0.9186	0.9078	0.9093	0.9136	0.9164	0.8730	0.8931	0.0022

Table 5: AUC and AP of TB-GCN and baselines on link prediction tasks for the networks in Table 2.

TREE+RGG, suggesting that TB-GCN is also suitable for the networks with tree-like structures.

Table 5 reports the best baselines to outperform TB-GCN on DISEASE-LP, BSM, RGG, WS, and SCALE-FREE. We analyze the relationship between a node’s degree and its neighbors’ degree. We consider denoting the average degree of k -degree nodes’ neighbors by $N(k)$ (Fig 4), and find that these networks’ $N(K)$ are close to linear functions. Therefore, we conjecture that HGCN works better on networks with non-linear $N(K)$. For these networks, the connecting behaviors of some nodes are featured by assortativity and some by disassortativity, for example, scientific coauthorship networks. We refer the readers to Ref. (Xie et al. 2018) for a thorough discussion of the transition phenomena of $N(K)$ for coauthorship networks.

6 Conclusion

We introduced a novel architecture TB-GCN that learns the trivial bundle embeddings for networks with or without node features using graph convolutional networks. TB-GCN represents both the assortativity and disassortativity in nodes’ preference of choosing which nodes to connect, a new perspective of finding a proper underlying geometry for networks. It achieves state-of-the-art or comparable performances on LP and NC tasks in comparison to the Euclidean and hyperbolic GCNs, suggesting its ability to learn geometric rep-

representations for networks, especially for the networks with some nodes' connecting behaviors featured by assortativity and some by disassortativity. We expect that non-trivial bundle embeddings can further increase the quality of bundle embeddings.

References

- Roy M Anderson and Robert M May. *Infectious diseases of humans: dynamics and control*. Oxford university press, 1992.
- Mikhail Belkin and Partha Niyogi. Laplacian eigenmaps and spectral techniques for embedding and clustering. In *NeurIPS*, volume 14, pages 585–591, 2001.
- Silvère Bonnabel. Stochastic gradient descent on riemannian manifolds. *IEEE Transactions on Automatic Control*, 58(9):2217–2229, 2013.
- Ines Chami, Zhitao Ying, Christopher Ré, and Jure Leskovec. Hyperbolic graph convolutional neural networks. *Advances in Neural Information Processing Systems*, 32:4868–4879, 2019.
- Inderjit S Dhillon and Suvrit Sra. Generalized nonnegative matrix approximations with bregman divergences. In *NeurIPS*, volume 18. Citeseer, 2005.
- Bhuwan Dhingra, Christopher J Shallue, Mohammad Norouzi, Andrew M Dai, and George E Dahl. Embedding text in hyperbolic spaces. *NAACL HLT*, 2018.
- George H Dunteman. *Principal components analysis*. Number 69. Sage, 1989.
- Octavian-Eugen Ganea, Gary Bécigneul, and Thomas Hofmann. Hyperbolic neural networks. *Advances in Neural Information Processing Systems*, pages 5345–5355, 2018.
- Rainer Gemulla, Erik Nijkamp, Peter J Haas, and Yannis Sismanis. Large-scale matrix factorization with distributed stochastic gradient descent. In *Proceedings of the 17th ACM SIGKDD International Conference on Knowledge Discovery and Data Mining*, pages 69–77, 2011.
- Albert Gu, Frederic Sala, Beliz Gunel, and Christopher Ré. Learning mixed-curvature representations in product spaces. In *International Conference on Learning Representations*, 2018.
- Çaglar Gulcehre, Misha Denil, Mateusz Malinowski, Ali Razavi, Razvan Pascanu, Karl Moritz Hermann, Peter Battaglia, Victor Bapst, David Raposo, Adam Santoro, et al. Hyperbolic attention networks. *International Conference on Learning Representations*, 2019.
- William L Hamilton, Rex Ying, and Jure Leskovec. Inductive representation learning on large graphs. In *Proceedings of the 31st International Conference on Neural Information Processing Systems*, pages 1024–1034, 2017.
- Sergey Ioffe and Christian Szegedy. Batch normalization: Accelerating deep network training by reducing internal covariate shift. In *International Conference on Machine Learning*, pages 448–456. PMLR, 2015.
- Diederik P Kingma and Jimmy Ba. Adam: A method for stochastic optimization. *International Conference on Learning Representations*, 2015.
- Thomas N Kipf and Max Welling. Semi-supervised classification with graph convolutional networks. *International Conference on Learning Representations*, 2017.
- Dmitri Krioukov, Fragkiskos Papadopoulos, Maksim Kitsak, Amin Vahdat, and Marián Boguná. Hyperbolic geometry of complex networks. *Physical Review E*, 82(3):036106, 2010.
- Daniel D Lee and H Sebastian Seung. Learning the parts of objects by non-negative matrix factorization. *Nature*, 401(6755):788–791, 1999.
- Jure Leskovec, Jon Kleinberg, and Christos Faloutsos. Graph evolution: densification and shrinking diameters. *ACM transactions on Knowledge Discovery from Data (TKDD)*, 1(1):2–es, 2007.
- Jure Leskovec, Daniel Huttenlocher, and Jon Kleinberg. Predicting positive and negative links in online social networks. In *Proceedings of the 19th International Conference on World Wide Web*, pages 641–650, 2010.

- Yujia Li, Daniel Tarlow, Marc Brockschmidt, and Richard Zemel. Gated graph sequence neural networks. *International Conference on Learning Representations*, 2016.
- Qi Liu, Maximilian Nickel, and Douwe Kiela. Hyperbolic graph neural networks. *Advances in Neural Information Processing Systems*, 2019.
- Alessandro Muscoloni, Josephine Maria Thomas, Sara Ciucci, Ginestra Bianconi, and Carlo Vittorio Cannistraci. Machine learning meets complex networks via coalescent embedding in the hyperbolic space. *Nature communications*, 8(1):1–19, 2017.
- Galileo Namata, Ben London, Lise Getoor, Bert Huang, and UMD EDU. Query-driven active surveying for collective classification. In *10th International Workshop on Mining and Learning with Graphs*, volume 8, page 1, 2012.
- Mark EJ Newman. Mixing patterns in networks. *Physical review E*, 67(2):026126, 2003.
- Maximilian Nickel and Douwe Kiela. Poincaré embeddings for learning hierarchical representations. *Advances in Neural Information Processing Systems*, 30:6338–6347, 2017.
- Maximilian Nickel and Douwe Kiela. Learning continuous hierarchies in the lorentz model of hyperbolic geometry. In *International Conference on Machine Learning*, pages 3779–3788. PMLR, 2018.
- Fragkiskos Papadopoulos, Constantinos Psomas, and Dmitri Krioukov. Network mapping by replaying hyperbolic growth. *IEEE/ACM Transactions on Networking*, 23(1):198–211, 2014.
- Frederic Sala, Chris De Sa, Albert Gu, and Christopher Ré. Representation tradeoffs for hyperbolic embeddings. In *International Conference on Machine Learning*, pages 4460–4469. PMLR, 2018.
- Rik Sarkar. Low distortion delaunay embedding of trees in hyperbolic plane. In *International Symposium on Graph Drawing*, pages 355–366. Springer, 2011.
- Prithviraj Sen, Galileo Namata, Mustafa Bilgic, Lise Getoor, Brian Galligher, and Tina Eliassi-Rad. Collective classification in network data. *AI magazine*, 29(3):93–93, 2008.
- Norman Steenrod. *The topology of fibre bundles. (PMS-14), Volume 14*. Princeton University Press, 2016.
- Alexandru Tifrea, Gary Bécigneul, and Octavian-Eugen Ganea. Poincaré glove: Hyperbolic word embeddings. *International Conference on Learning Representations*, 2019.
- Petar Veličković, Guillem Cucurull, Arantxa Casanova, Adriana Romero, Pietro Lio, and Yoshua Bengio. Graph attention networks. *International Conference on Learning Representations*, 2017.
- Li Wan, Matthew Zeiler, Sixin Zhang, Yann Le Cun, and Rob Fergus. Regularization of neural networks using dropconnect. In *International Conference on Machine Learning*, pages 1058–1066. PMLR, 2013.
- Zuxi Wang, Yao Wu, Qingguang Li, Fengdong Jin, and Wei Xiong. Link prediction based on hyperbolic mapping with community structure for complex networks. *Physica A: Statistical Mechanics and its Applications*, 450:609–623, 2016.
- Zheng Xie. A topic detection method based on word-attention networks. *Journal of Data and Information Science*, page 20210810, 2021.
- Zheng Xie, Zhenzheng Ouyang, Jianping Li, Enming Dong, and Dongyun Yi. Modelling transition phenomena of scientific coauthorship networks. *Journal of the Association for Information Science and Technology*, 69(2):305–317, 2018.
- Keyulu Xu, Weihua Hu, Jure Leskovec, and Stefanie Jegelka. How powerful are graph neural networks? *International Conference on Learning Representations*, 2019.
- Zhilin Yang, William Cohen, and Ruslan Salakhudinov. Revisiting semi-supervised learning with graph embeddings. In *International Conference on Machine Learning*, pages 40–48. PMLR, 2016.
- Rex Ying, Ruining He, Kaifeng Chen, Pong Eksombatchai, William L Hamilton, and Jure Leskovec. Graph convolutional neural networks for web-scale recommender systems. In *Proceedings of the 24th ACM SIGKDD International Conference on Knowledge Discovery & Data Mining*, pages 974–983, 2018.
- Hongyi Zhang, Sashank J Reddi, and Suvrit Sra. Riemannian svrg: Fast stochastic optimization on riemannian manifolds. *Advances in Neural Information Processing Systems*, 29:4592–4600, 2016.
- Yiding Zhang, Xiao Wang, Chuan Shi, Xunqiang Jiang, and Yanfang Fanny Ye. Hyperbolic graph attention network. *IEEE Transactions on Big Data*, 2021.

Hongmin Zhu, Fuli Feng, Xiangnan He, Xiang Wang, Yan Li, Kai Zheng, and Yongdong Zhang. Bilinear graph neural network with neighbor interactions. *Proceedings of the Twenty-Ninth International Joint Conference on Artificial Intelligence* (, pages 1452–1458, 2020).